Construction and Building Materials 131 (2017) 334–346

Contents lists available at ScienceDirect

Construction and Building Materials

journal homepage: www.elsevier.com/locate/conbuildmat

Evaluation of slag characteristics on the reaction kinetics and mechanical properties of Na_2CO_3 activated slag

B. Yuan [a,b], Q.L. Yu [a,*], H.J.H. Brouwers [a,b]

[a] Department of the Built Environment, Eindhoven University of Technology, P.O. Box 513, 5600 MB Eindhoven, The Netherlands
[b] State Key Lab of Silicate Materials for Architectures, Wuhan University of Technology, Wuhan 430070, PR China

HIGHLIGHTS

- Slag characteristics on Na_2CO_3 activated slag are explored.
- Na_2CO_3 activation is considerably accelerated by controlling slag characteristics.
- Increasing the slag fineness enhances only the early age strength.
- Na_2CO_3 dosage (3–5 wt.%) on strength and reaction kinetics is not prominent.

ARTICLE INFO

Article history:
Received 11 July 2016
Received in revised form 24 August 2016
Accepted 14 November 2016

Keywords:
Sodium carbonate
Ground granulated blast furnace slag
Fineness
Reaction kinetics
Compressive strength

ABSTRACT

This paper evaluates the slag characteristics on the reaction kinetics, reaction products and mechanical properties of sodium carbonate activated slag (SCAS). The results show that, by reducing the slag particle size, the precipitation of strength-giving phase of SCAS can be dramatically accelerated, and the time to reach the reaction peak (TRRP) can be accelerated from 86 h to 23 h and a 3 d-compressive strength of about 34 MPa is achieved. The fresh behaviour of pastes is affected by the initial precipitation of calcium carbonate and the formation of gaylussite is also accelerated when reducing the particle sizes of slags. It is observed that the early strength development of samples is largely controlled by the fineness of slag particles, while the later strength firstly increases with the reduction of slag particles until reaching a turning point and then decreases. Furthermore, the influential factors including the alkali activator dosage and slag characteristics on the reaction kinetics of Na_2CO_3 activated slag are discussed.

1. Introduction

Though Portland cement (PC) has been confirmed to be a reliable building material, the production of cement, however, involves relatively high energy-consumption and gas-emission [1]. Over the past decades, as an alternative binder to PC, alkali activated slag (AAS) has attracted extensive attention as it is generally associated with ambient temperature curing and excellent materials properties [2–5]. It is known that alkali natures [6–8], alkali concentrations [9], reactivity and physiochemical properties of raw materials [10–13] and curing methods [14,15] can significantly affect the performance of AAS. The influential factors of waterglass activation have been extensively investigated due to its benefits in terms of mechanical properties [16] and durability [5], including waterglass dosages, waterglass modulus, water content, blended binders (mostly among slag, fly ash and metakaoline) and curing methods [5,15–18], etc. However, the relatively short setting time [8,19] and large drying shrinkage [20,21] of waterglass activated slag negatively affect its practical application.

Different manufacturing process, such as cooling methods and original materials of slag production, can lead to significant difference concerning chemical compositions and reactivity, and consequently different materials performance of AAS [22–25]. El-Didamony et al. [23] studied the mechanical properties and durability of waterglass activated GGBS blended with air-cooled slag, and found that the incorporation of air-cooled slag decreases the strength to some extent. Compared to the widely used GGBS in OPC or AAM, the utilization of steel-making slag is still limited to a much lower level [22,25]. By investigating three silicate-activated slags (AAS) with varying MgO contents, Bernal et al. [24] concluded that a high content of MgO in slag can increase the extent of reaction, forming more secondary phase hydrotalcite which enhances the carbonation resistance of AAS.

* Corresponding author.
E-mail address: q.yu@bwk.tue.nl (Q.L. Yu).

http://dx.doi.org/10.1016/j.conbuildmat.2016.11.074
0950-0618/

Table 1
Summary of the recipes and performances of Na_2CO_3 activated GGBS in literatures.

References	Designed parameters	Descriptions	Notes
Bernal et al. [30]	Na_2CO_3 = 8 wt.% Slag fineness = 410 ± 10 m^2/kg 0.1–74 μm with d50 of 15 μm W/B* = 0.40	$f_{Comp.7\ d}$ = 31 MPa $f_{Comp.28\ d}$ = 38 MPa Calorimetry, TRRP = ~125 h	Demoulded after 4 d of curing
Jimenez et al. [8]	Na_2CO_3 = 3 wt.% of Na_2O Slag fineness = 460 m^2/kg W/B* = 0.51	Calorimetry, TRRP = ~137 h	Initial setting time >3 d
Abdalqader et al. [32]	$Na_2CO_3^*$ = 5 and 10 wt.% Slag fineness = 545 m^2/kg W/B* = 0.31	5%, $f^*_{Comp.3\ d}$ = 38 MPa $f_{Comp.28\ d}$ = 45 MPa 10%, $f_{Comp.3\ d}$ = 25 MPa $f_{Comp.28\ d}$ = 60 MPa Calorimetry, TRRP* = 45 ~50 h	Demoulded after 2 d of curing
Jin et al. [33]	Na_2CO_3 = 4, 6 and 8 wt.% Slag fineness = 493 m^2/kg W/B* = 0.32	4%, $f_{Comp.3\ d}$ = 5 MPa $f_{Comp.28\ d}$ = 34 MPa 6%, $f_{Comp.3\ d}$ = 11 MPa $f_{Comp.28\ d}$ = 42 MPa 8%, $f_{Comp.3\ d}$ = 39 MPa $f_{Comp.28\ d}$ = 62 MPa	Demoulded after 1 d of curing
Kovtun et al. [36]	Na_2CO_3 = 3.5 wt.% of Na_2O Slag fineness = 425 m^2/kg 0.4–152 μm with d50 of 17 μm W/B* = 0.26	$f_{Comp.28\ d}$ = 55 MPa $f_{Comp.91\ d}$ = 58 MPa	Concrete Initial setting time = 455 min
Zivica [18]	Na_2CO_3 = 3, 5 and 7 wt.% Slag fineness – Not Mentioned W/B* = 0.31	Initial setting time (Mortar) 3%, 01:00 h 5%, 01:00 h 7%, 00:40 h	
Atis et al. [28]	Na_2CO_3 = 4, 6 and 8 wt.% of Na Slag fineness = 425 m^2/kg W/B* = 0.5	Mortar 4%, $f_{Comp.7\ d}$ = 16.8 MPa $f_{Comp.28\ d}$ = 24.7 MPa 6%, $f_{Comp.7\ d}$ = 21.7 MPa $f_{Comp.28\ d}$ = 27.6 MPa 8%, $f_{Comp.7\ d}$ = 26.7 MPa $f_{Comp.28\ d}$ = 35.7 MPa	Initial setting time (Pastes) 4%, 190 min 6%, 180 min 8%, 170 min
Jimenez et al. [7]	Na_2CO_3 = 3 and 4 wt.% of Na_2O Slag fineness = 450 and 900 m^2/kg W/B* = 0.51 and 0.61	450 m^2/kg (0.51), 3 wt.% Na_2O: $f_{Comp.3\ d}$ = 30 MPa $f_{Comp.28\ d}$ = 42 MPa 4 wt.% Na_2O: $f_{Comp.3\ d}$ = 42 MPa $f_{Comp.28\ d}$ = 50 Mpa 900 m^2/kg (0.61), 3 wt.% Na_2O: $f_{Comp.3\ d}$ = 24 MPa $f_{Comp.28\ d}$ = 42 MPa 4 wt.% Na_2O: $f_{Comp.3\ d}$ = 40 MPa $f_{Comp.28\ d}$ = 56 MPa	Cured at 25 °C

On the other hand, sodium carbonate activated slag (SCAS) has also been widely investigated during the last decades, however, in most cases for comparative purposes [8,18,26–29]. In the few available literatures [8,30], a prolonged reaction process is often reported, i.e. it generally takes approximate 3–5 d before it can be demoulded depending on the designed recipe. The further reaction is considered to be a cyclic reaction process with a buffered alkali environment controlled by carbonate anions maintained by the continuous dissolution of $CaCO_3$ [31]. A recent research [30] indicates that the delayed reaction process of Na_2CO_3 activated slag is mostly attributed to the precipitation of $CaCO_3$ and consumption of CO_3^{2-} anions provided by the activator. However, it should be noted that samples activated by Na_2CO_3 with fast setting time are also reported [7,32,33], while the reasons were rarely explained. Jin et al. [33] reported 3 d–compressive strengths of 5–39 MPa while the samples were demoulded after 1 d of curing. Abdalqader et al. [32] recorded the time to reach the reaction peak (TRRP) of 45–50 h with 3 d-compressive strengths of 25–38 MPa and the samples were demoulded after 2 d of curing. Jimenez et al. [7] also reported 3 d-compressive strengths of 24–42 MPa. Table 1 briefly summarizes the reaction and performance of sodium carbonated activation. However, it is difficult to compare these results or sometimes the results are controversial because of the complex influential factors, e.g. chemical compositions or fineness of raw materials, alkali dosage, water to solid ratio or curing method/temperature.

Only a few researches have studied the factors affecting the reaction kinetics, mechanical properties and durability of SCAS. By increasing the alkali concentration [28], mixing with NaOH [34,35] or incorporating waterglass [26], blending with reactive admixtures (e.g. MgO [32] and lime [36]), the reaction kinetics of SCAS can be accelerated to certain degrees. Nevertheless, all of these methods are either inefficient or costly or having side effects. For example, by adding NaOH to the activator, the sample can obtain a 1 d-compressive strength of about 8 MPa, while nearly no further strength development after 7 d of curing is observed

Table 2
Chemical composition, density and Blaine fineness of GGBSs investigated.

Chemical compositions (%)	Slag-1	Slag-2	Slag-3	Slag-1G
SiO_2	34.61	30.24	30.23	Same to Slag-1
CaO	37.63	40.68	40.51	
Al_2O_3	13.26	12.67	12.58	
MgO	9.94	9.05	9.05	
Fe_2O_3	0.47	0.64	0.60	
SO_3	1.24	3.53	3.47	
K_2O	0.47	0.38	0.43	
TiO_2	0.98	1.49	1.48	
Cl	0.01	0.05	0.03	
L.O.I	−0.46	−0.36	−0.33	
Blaine fineness (m^2/kg)	373	436	461	722
Specific density (kg/m^3)	2930	2930	2920	2910

[34,37]. Until recently, by using calcined layered double hydroxides, Ke et al. [38] accelerated the reaction of sodium carbonate activated slag by removing the carbonate anions which consequently yield a significant rise in pH and the samples can be hardened within 24 h. However, its effect on the strength development was not yet investigated.

Up till now, limited attention has been paid to the effect of the physical properties of raw materials, such as slag fineness. For waterglass activated slag, when reaching a critical value (400 m^2/kg [39] or 450 m^2/kg [16]) the fineness makes no effect on the strength development. Most recently, Lee et al. [40] studied the influence of slag fineness on the mechanical properties of slag-fly blenders activated by waterglass, and found that early age strength ($\leqslant$7 d) increased with the increase of slag fineness. However, a reduction on the 28 d strength was observed probably due to the formation of micro-cracks induced by the incorporation of fine slag particles. Jimenez et al. [7] studied the effect of slag fineness on the mechanical properties of SCAS and reported that the influence is not significant. However, to the authors' knowledge, the slag fineness on the reaction kinetic of SCAS has not been investigated. As discussed by Bernal et al. [30], the availability of CO_3^{2-} anions in the pore solution plays a significant role on the reaction kinetics. By reducing the slag particle sizes, more Ca^{2+} ions can be dissolved at the early stage which will be precipitated with CO_3^{2-} anions, and thus potentially the slow reaction/setting of SCAS can be solved to some extent.

This research aims to study the slag characteristics on the reaction kinetics and strength development of slag activated by sodium carbonate. Four slags with different fineness and three different Na_2CO_3 contents (3–5% Na_2O by mass of slag) were applied. Since extensive researches have been paid to the activation effect of waterglass, as a comparative purpose to sodium carbonate activation, the reaction kinetics of waterglass activated products were also studied and analyzed to check the influence of slag fineness. The raw materials are characterized, including X-ray fluorescence (XRF), X-ray diffractometry (XRD), particle size distribution (PSD), density, loss on ignition (L.O.I.), and Blaine specific surface area. Applying the isothermal calorimetry, XRD, Fourier transform infrared spectroscopy (FT-IR), thermogravimetric analysis (TGA) and compressive strength test at different curing ages, the designed mixtures are characterized and analyzed.

2. Materials and experiments

2.1. Materials

Three ground granulated blast furnace slags (GGBS) were studied (supplied by ENCI B.V, the Netherlands). The coarsest slag was also ground to be the finest slag, and the obtained slag is designated as Slag-1G. Detailed information about the slags will be discussed in Section 3.1. Sodium carbonate (powder, analytical grade) was applied as the activator in this study with different concentrations. All the designed activators (Table 3) were firstly mixed/dissolved in water followed by cooling down to room temperature (20 ± 1 °C) prior to further actions.

Table 3
Mix proportions of specimens.

Activators	Series	Numbers	Series				W/S
			A	B	C	D	
			Slag-1	Slag-2	Slag-3	Slag-1G	
Sodium Carbonate (Na_2CO_3)	S	3	3%	3%	3%	3%	0.4
		4	4%	4%	4%	4%	
		5	5%	5%	5%	5%	
Waterglass	W	–	4%	4%	4%	4%	

2.2. Experiments

According to the different slags or activators applied, the specimens are divided into different series as shown in Table 3. The definition of mixtures is depending on the fineness of slag, types and concentrations of activators and concentrations. For example, mixture AS3 means Slag-1 ("A") activated by sodium carbonate ("S") with the dosage of 3 wt.% ("3") (equivalent Na_2O by mass of slag), and mixture series S means samples activated by sodium carbonate. Accordingly, mixture series AW is Slag-1 activated by waterglass.

2.2.1. Fresh behaviour

Following the EN 1015-3: 2007, the flowability of the designed mixtures was measured with a Hägermann cone (top diameter = 70 mm, base diameter = 100 mm, height = 50 mm). The fresh samples were firstly filled into the Hägermann cone and after about 15 s the Hägermann cone was lifted vertically and the diameters of the resulted paste spread were measured along two perpendicular directions. The average diameter is interpreted as the flowability of the pastes.

Besides, after mixing, the solution of the fresh pastes with the coarsest slag particles was extracted by a centrifugal at the very early age (0.5 h and 3 h after mixing). Subsequently, the calcium ion concentration was measured by an ion chromatography (Thermo Scientific™).

2.2.2. Isothermal calorimetry

The heat release of samples activated by different activators was measured by a calorimetry instrument set at 20 °C (TAM AIR Calorimeter). It should be noted that the initial 4–6 min after mixing could not be measured due to the sample preparation procedure and the initial 0.5–1 h of the recorded data could be inaccurate because of the instability of instrument disturbed by the loading process. The results were normalized by the mass of solid, excluding the water amount.

2.2.3. X-ray diffractometry

X-ray diffractometry (XRD) analysis was performed by using a Cu tube (40 kV, 30 mA) with a scanning range from 3° to 55° 2 θ, applying a step 0.02° and 5 s/step measuring time. The qualitative analysis was carried out by using the Diffrac^{plus} Software (Bruker AXS) and the PDF database of ICDD.

2.2.4. FT-IR

The FT-IR spectra of the reaction products were collected using a PerkinElmer Frontier™ MIR/FIR Spectrometers using the

attenuated total reflection (ATR) method (GladiATR). All spectra were scanned 48 times from 4000 to 400 cm^{-1} at a resolution of 4 cm^{-1}.

2.2.5. TGA

Thermogravimetry analyses (TGA) were also applied to analyze the reaction degree of alkali-activation at different curing ages. The samples were firstly ground and then the fineness was controlled by using a 63 μm sieve. To check the reaction products of samples from a finer slag at the early ages, mixture CS5 is selected, the samples were firstly held isothermally at 20 °C for 3 h to stabilize the internal balance of TG instrument and then heated up to 1000 °C at the rate of 1 °C/min. While the other samples of assessing the amount of chemically bound water were firstly heated up to 105 °C and held isothermally for 3 h, then up to 1000 °C and held isothermally for 3 h, both at the rate of 10 °C/min. Nitrogen was used as the carrier gas with the rate of 40 ml/min during the TGA measurements.

2.2.6. Compressive strength

The starting raw materials were mixed with the designed activators in a mortar mixer following the preparation procedure suggested by EN 196-1 [41]. Samples were cast into the plastic moulds ($40 \times 40 \times 160$ mm^3) followed by a manual vibration. Afterwards, plastic foils were applied to seal the surface of the specimens to prevent the moisture loss. Because of the different reaction rates cured at ambient temperature (20 ± 1 °C), the samples were plastic cover-cured until the age of testing. The compressive strength of the specimens was determined according to EN 196-1 [41].

3. Results and discussion

3.1. Physical characterization of slags

Table 2 shows the properties of slag-1–3 and slag-1G. As can be seen, Slag-2 and Slag-3 show similar contents of the main elements, including Ca, Al, Si and Mg, while Slag-1 gives a higher content of SiO_2 and MgO but lower content of CaO. However, the differences are relatively small as they are all manufactured following the same procedure. Table 4 summarizes the chemical composition of different blast furnace slags reported in previous literatures about sodium carbonate-activation products [7,8,18,28,30,32,33,36]. In general, the oxide compositions of these slags are within the range of: SiO_2 33–41%, CaO 39–43%, Al_2O_3 (except Ref [18], 7.32%) 11–15%, MgO 5–12% and Fe_2O_3 <1.2%. Besides, Reinhardt [42] also reported that the typical range of chemical compositions of GGBS are: SiO_2 28–48%, CaO 35–48%, Al_2O_3 6–17%, MgO 2–11% and SO_3 0.8–3.0%. In sum, the chemical compositions of the present slags are similar to the previous studies and with a medium content of MgO, which could potentially induce the formation of the secondary phase hydrotalcite and increase the extent of reaction degree of alkali activation [24].

The particle size distributions and SEM images of these slags are presented in Figs. 1 and 2, respectively. It is clear that Slag-1 is the coarsest and Slag-1G is the finest one, while Slag-2 and Slag-3 possess similar medium sizes but the former one is slightly finer. On the other hand, by grinding materials the morphology of slag particles is changed from irregular shape to broken particles as shown in Fig. 2 (Slag-1 and Slag-1G), which could potentially change the reactivity. Table 2 gives the Blaine specific surface area of these slags ranging from 373 to 722 m^2/kg. In the previous researches, only few researches have presented the particles sizes distribution of the used slags [30,36] for the sodium carbonate activation as shown in Table 1, increasing the difficulties to effectively compare these results. Nevertheless, the Blaine fineness of slags was generally characterized, and the fineness were mostly in the range of 410–460 m^2/kg, which is similar to that of Slag-2 and Slag-3.

The effect of alkali activation can be significantly influenced by the chemistry of alkali activators and characteristics of raw materials. In this research, four slags were applied as the sole binder (Table 3). Based on the characterized results and compared to the previous studies [7,8,18,28–30,32,33,36], it is clear that all slags show similar contents of chemical compositions, while the main difference is related to their physical properties, i.e. particle size/fineness.

3.2. Reaction kinetics

Fig. 3 shows the heat evolution of the designed mixtures. As can be seen, the heat release curves are similar as Portland cement based materials [43] or slag activated by sodium silicate [17,24]. A pre-induction period (first/initial dissolution of slag particles) is generally observed during the initial 0.5 h, followed by an induction period with different lengths depending on the slag fineness and alkali activators applied. Afterwards, corresponding to the major formation/precipitation of strength-gaining phase, an intensive acceleration period and deceleration period (main reaction peak) are shown. Furthermore, for samples activated by sodium carbonate, an additional peak is observed at approximate 1 h after mixing, which could potentially be assigned to the initial precipitation of calcium carbonate [26].

A lengthened dormant period (DP) of up to around 2 d is observed for samples with the coarsest slag (Mixture series AS) (see Fig. 3a for the definition of time to reach the reaction peak (TRRP), DP and relative setting time (RST) and Table 3 for the mixtures design). The strength-giving phases are generally precipitated after 3 d, which corresponds to the phenomenon that most samples remain unhardened after 2–3 d of curing. This is also confirmed by other researches [8,30,32]. Jimenez and Puertas [8] reported a dormant period of around 100 h of Na_2CO_3 activated slag cement with alkali concentration of 3 Na_2O.% by mass of slag

Table 4
Summary of chemical compositions of GGBS in literatures.

References		Chemical compositions (%)						
		SiO_2	CaO	Al_2O_3	MgO	Fe_2O_3	SO_3	L.O.I
Bernal et al. [30]		33.8	42.6	13.7	5.3	0.4		1.8
Jimenez et al. [8]		34.47	40.3		11.8			
Abdalqader et al. [32]		36.79	39.24	11.51	8.1	0.42	1.03	
Jin et al. [33]		37	40	13	8		2.5	
Kovtun et al. [36]		34.87	37.05	14.38	8.03	0.89	1.96	0.16
Zivica [18]		40.19	42.1	7.32	8.06	1.16	0.8	0.3
Atis et al. [28]		36.7	32.61	14.21	10.12	0.98	0.99	
Jimenez et al. [7]	450 m^2/kg	35.50	41.45	12.15	8.34	1.01	2.47	
	900 m^2/kg	34.72	41.05	11.87	8.24	0.44	2.43	

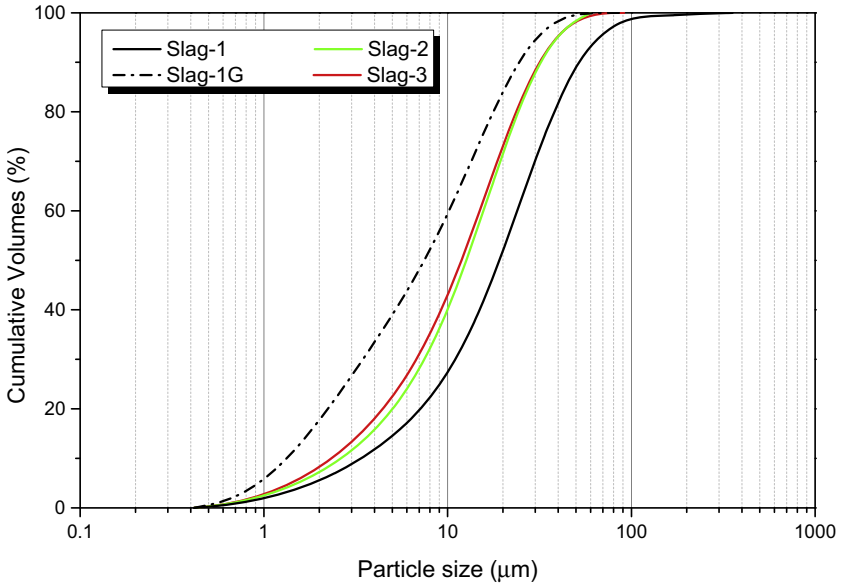

Fig. 1. Particle size distributions of slags.

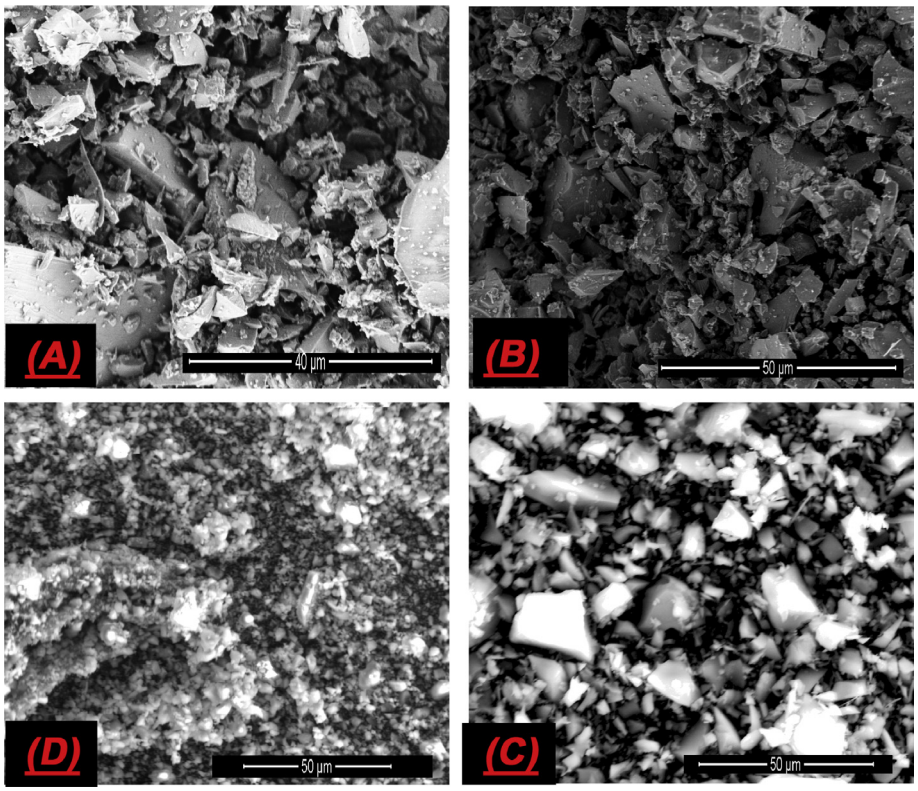

Fig. 2. SEM pictures of anhydrous slags: (A) slag-1, (B) slag-2, (C) slag-3 and (D) slag-1G.

and a water/binder ratio of 0.51. A similar result was also observed by Bernal et al. [30] who found an induction period of about 62 h with 8 wt.% of Na_2CO_3 by mass of slag and a water to binder ratio of 0.4. With higher alkali contents (5% and 10%) and a lower water to binder ratio (0.31), Abdalqader et al. [32] reported a faster reaction rate with TRRP up to approximate 48 h after casting. Via analyzing the aged sodium carbonated activated products and fresh pastes at different curing ages, Bernal et al. [30] proposed a conceptual reaction model of sodium carbonate activated slag, suggesting that the initially chemically precipitated $CaCO_3$ is the main reason for the delayed reaction. On the other hand, with a high alkali content Mix AS5 shows a relatively high heat release (peak height) and a short time to reach the reaction peak (TRRP), while lowering the alkali dosage to 4% or 3% the difference is minimized, as shown in Fig. 3 (Mix AS3 and 4).

By reducing the slag particle size, both the reaction intensity and TRRP are accelerated as depicted in Fig. 3, especially the TRRP dramatically shifted from 67 to 87 h to 25–40 h. In general,

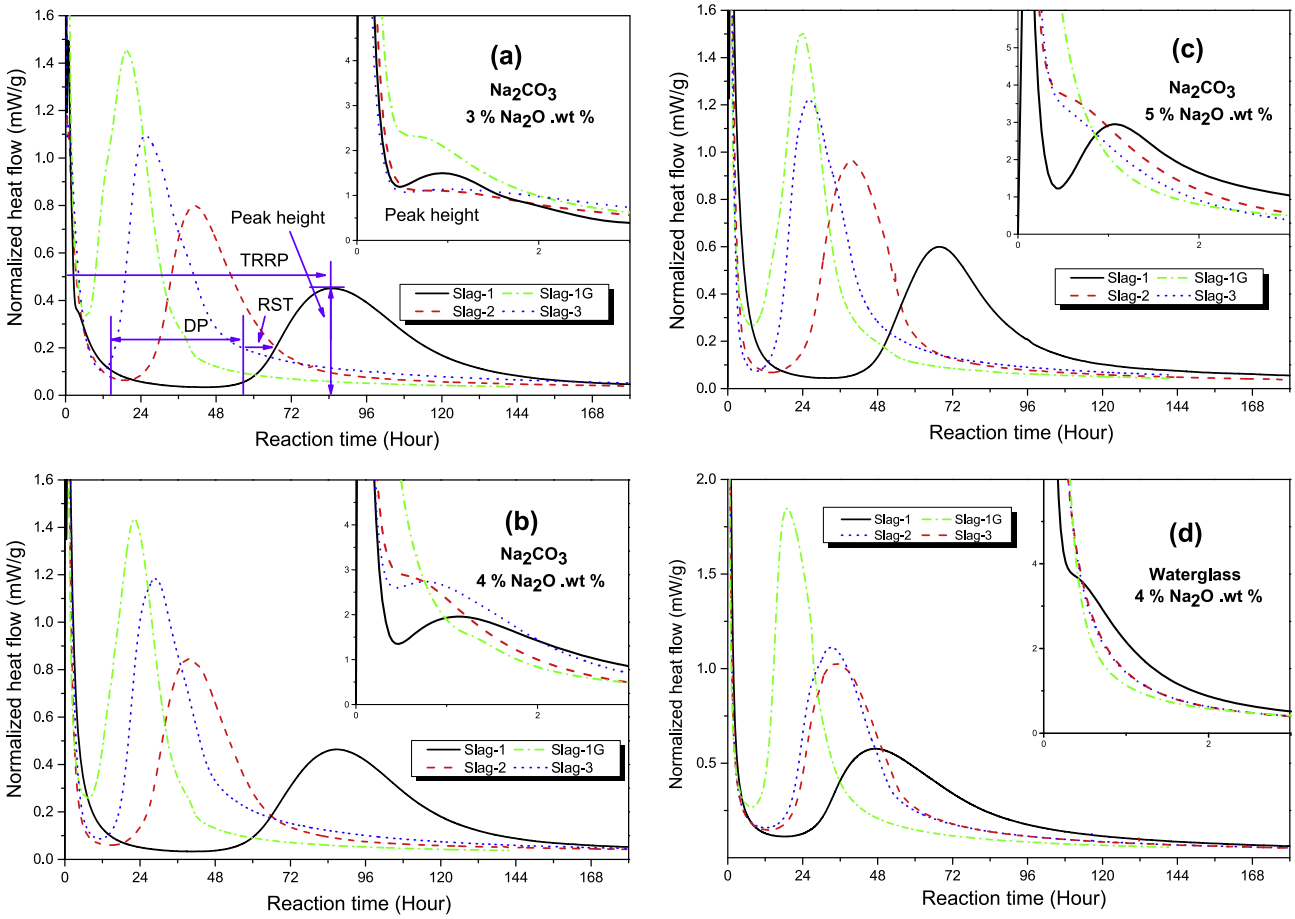

Fig. 3. Heat evolutions of sodium carbonate activated slags with different Na_2O. wt.% dosages (by mass of slag): (a) 3%, (b) 4% and (c) 5%, and (d) waterglass activated slags. (TRRP is time to reach the reaction peak, DP is the dormant period and RST is the relative setting time).

Mixture series CS (Table 3) show a faster reaction rate than Mixture series BS, which corresponds to the particle sizes of these two slags. It is clear that the alkali dosage mainly influences the intensity of heat evolution, while its effect on the TRRP is not prominent. In the previous research, a relatively fast reaction process of SCAS was also reported [33]. However, the reason for this phenomenon was not investigated. In the present research, the possible reasons for the accelerated reaction and its influential factors are studied.

Fig. 3d presents the heat release of slags activated by waterglass. As can be seen, mixture CW (Table 3) shows a slightly faster and higher intensity reaction than mixture BW, while mixture AW gives a relatively slow reaction and low intensity. It is obvious that the fineness of slags can significantly affect the reaction of waterglass activation. However, the influence of slag fineness is not as obvious as observed in SCAS. The previous reports show that after reaching a critical value (400 m^2/kg [37] or 450 m^2/kg [16]), the fineness of slag will have no effect on the alkali activation effect. Applying an alkali dosage of 5% (modulus 1.5), Ravikumar and Neithalath [17] reported a faster reaction with the TRRP of around 19 h and a higher intensity of peak height of around 2.5 mW/g. It should also be noted that, besides alkali dosage and slag fineness, the silica modulus can also influence the waterglass activation. Gao et al. [44] studied the waterglass modulus on the reaction kinetics of samples with slag/fly ash blends and reported TRRPs of around 12 h with an alkali content of 5.6 Na.% by mass of slag and a water to binder ratio of 0.35. Depending on the proportion of waterglass applied, the reaction rate varies. Nevertheless, reported researches provide an indication about the effect of slag fineness on the reaction kinetics.

To eliminate the differences caused by the chemistry of raw slag, Slag-1G was applied following the same recipes and the results are shown in Fig. 3. In comparison with the other sodium carbonate activated products, Mix series DS (Table 3) show a relatively faster reaction rate (TRRP <24 h) and a higher intensity (1.4–1.5 mW/g), while the differences caused by the alkali nature are relatively small. Reversely, high dosages of sodium carbonate lead to slower reaction rates, which differs from the observation above and other published results [30,32]. Moreover, no clear peak at around 1 h after mixing is shown compared to the other sodium carbonate activated slags. It should be noted that mixture DW shows a similar TRRP as mixture DS5, indicating the alkali nature is not prominent in this range.

Fig. 4 summarizes the results discussed above. It clearly shows that by increasing the slag fineness, the reaction of TRRP and intensity (peak height) can be significantly improved, indicating that the slag fineness dominates the reaction kinetics of sodium carbonate activated slag. However, the effect of alkali dosages on the reaction is not prominent.

3.3. Fresh behaviour

The spread flow of the mixtures with a water-to-solid ratio of 0.4 was measured and the results are shown in Fig. 5. It is clear that

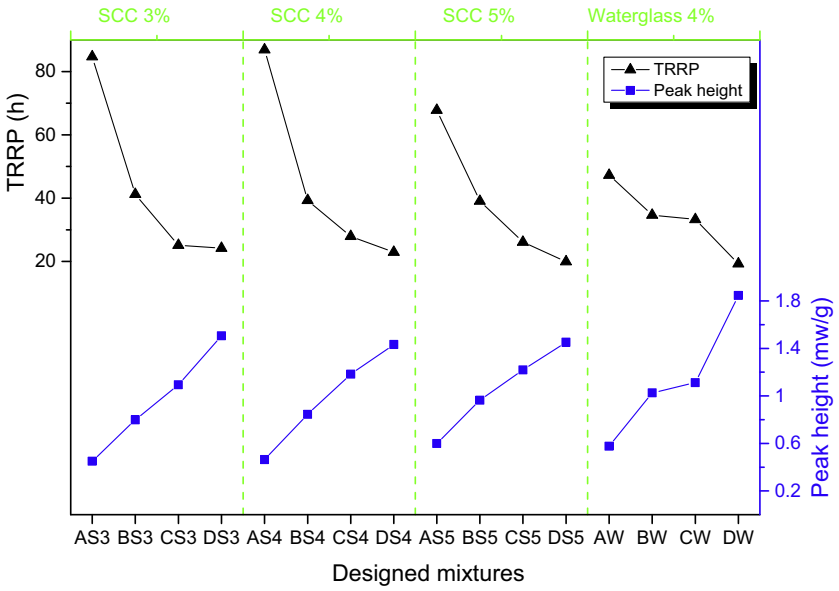

Fig. 4. Summarized results of TRRP (time to reach reaction peak) and peak height (intensities) for different mixtures (Table 3).

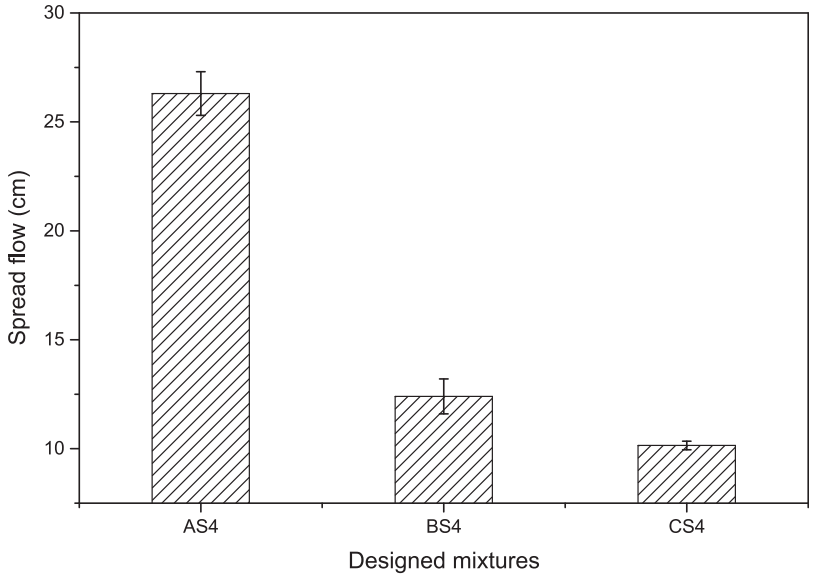

Fig. 5. Flowability of mixtures AS4, BS4 and CS4 (Table 3, the flow of DS4 was zero).

the flowability of the mixtures drops dramatically from high (Mixture AS4) to low (Mixture BS4) and then to approximately zero flowability (Mixture CS4). It is clear that the fineness of slag particles determines the spread flow as a high specific surface area leads to a high water demand. Rashad et al. [45] also studied the effect of the slag fineness on the mini flow of sodium sulfate activated slag, and found the flowability is mainly influenced by the particle sizes of slag while the effect of alkali dosages is not prominent. Yang and Song [46] investigated the workability of mixtures with different alkali contents and reported that the initial flow of produced mortar only slightly decreased with an increase of alkali content.

On the other hand, the effect of water to solid (W/S) ratios and sodium carbonate content on the flowability of samples has been investigated and it is logical to find that the flowability of pastes increases with the increase of W/S ratios but decreases with the increase of alkali content [47]. It is clear that finer particles demand more water due to the high specific surface area and consequently lead to a faster reaction but a lower flowability if the water dosage is fixed. However, it should be cautious that the initial precipitation of calcium carbonate could also potentially affect the fresh behaviour of sodium carbonate activated slag as the saturation limit of $CaCO_3$ is very low while the CO_3^{2-} anions concentration is high [30]. To further study its effect, the calcium concentration in the pore solutions extracted by a centrifugal of sodium carbonate activated slag at the initial 0.5–3 h after mixing was measured, and the results show that after 0.5 h, the Ca^{2+} concentration (0.28 mg/L) is slightly higher than that of 3 h (0.22 mg/L). Corresponding to the initial concentration of CO_3^{2-} anions, the saturation limit of $CaCO_3$ is already reached after 0.5 h of mixing, indicating the initial precipitation of $CaCO_3$ is influencing the workability of fresh pastes. In this case, except the increasing water demand, the initial precipitation of calcium carbonate is also

responsible for the dramatically decrease of the spread flow when increasing the slag fineness.

3.4. Mechanical properties

Fig. 6 presents the compressive strength of the designed mixes at the curing ages of 3 d, 7 d and 28 d, respectively. At low dosages (3%) of sodium carbonate activation, a higher alkali content and a finer raw material lead to a better mechanical performance. In the case of higher dosages (4 and 5%), the compressive strength firstly increases with the decrease of slag particles and then slightly decreases when the slag fineness reaches a critical point. Depending on the slag fineness and sodium carbonate dosages, the compressive strength of samples ranges between 0 and 33.9 MPa, 29.2–44.4 MPa, 36.5–56.1 MPa at the curing ages of 3 d, 7 d and 28 d, respectively, while those mixtures activated by waterglass show relatively higher strength ranging from 53.9 MPa to 79.4 MPa at different ages.

It should be noted that the Mix series AS (Table 3) show a very slow reaction rate (a virtual value is fabricated to give an indication of 3 d strength, as shown in Fig. 6). Nevertheless, the strength develops subsequently rather fast and the tested results are around 30–40 MPa at 7 d. A similar strength development was also reported by Bernal et al. [30] who used 8% of Na_2CO_3 by mass of slag as the activator and a water-to-binder ratio of 0.4, and observed a 4 d-compressive strength of 9 MPa followed by a dramatic increase to 31 MPa and 44 MPa at 7 d and 44 d, respectively. On the other hand, Mix series BS (Table 3) show a slightly faster strength development than Mix series CS at higher dosages, while at lower dosages the difference is negligible. In general, the compressive strength of Mix series BS&CS is slightly higher than the reported results from available literature [28,32]. The reasons could be mainly related to the particle sizes of slags.

As for Mix series W (Table 3), it is clear that the fineness of slags does not influence the strength development as these samples show similar compressive strength at different curing ages. Extensive concerns have been paid to the chemical properties of binders and activators of alkali activated slags [8,17,35], while the physical properties of starting materials are rarely reported [16,39]. In general, finer particles can dissolve faster than coarser particles under the same conditions, leading to a faster reaction and better material properties. Wang et al. [16] studied the effect of slag fineness on the strength development of alkali activated products, and found that the strength increases with the increase of slag fineness to some extent and then decreases after reaching the optimal value. However, the effect of slag fineness on the later strength development is not prominent. Besides, Shi and Li [39] also concluded that when the slag fineness reaches a critical value (400 m^2/kg), it will have no effect on the strength development (28 d).

To conclude, within the range of investigated slag fineness, the slag fineness shows a significant effect on the strength development of sodium carbonate activation especially at the early age, and the strength increases with the increase of slag fineness until reaching a turning point (in this study 436 m^2/kg).

3.5. Reaction products characterization

In previous research [48], we have characterized the reaction products of sodium carbonate activated slag with a coarse slag (mixture AS5) (Table 3) and confirmed that the initial formation of C-(A)-S-H gel starts after around 2–3 d of curing. In the current study, as shown in Fig. 7, the reaction products of samples with finer slags (mixture CS5) were characterized by XRD, FT-IR and TGA at the curing ages of 1 d and 2 d. It is clear that after 1 d of casting, the main reaction products of mixture CS5 are calcite (PDF # 00-47-1743) and gaylussite (PDF # 01-74-1235), while C-(A)-S-H gel is poorly crystalized and its reflections are overlapped with calcite as shown in Fig. 7a. When the curing time comes to 2 d, the main reaction products remain the same while the intensity of calcite/C-(A)-S-H gel increases dramatically. It should be noted that the formation of gaylussite occurs much earlier than samples applying coarser slag particles [48] which happened after 2 d of curing.

The FT-IR spectra of anhydrous slag-3 and mixture CS5 at the ages of 1 and 2 d are presented in Fig. 7b. The raw slag shows a broad band centred at approximate 891 cm^{-1} and 674 cm^{-1} which can be assigned to the vibration of Si-O bands in the SiO_4 groups and Al-O bands in the AlO_4 groups, respectively, while the weak bands around 1455 cm^{-1}, 871 cm^{-1} and 717 cm^{-1} are the vibration of $\upsilon_3[CO_3^{2-}]$, $\upsilon_2[CO_3^{2-}]$ and $\upsilon_4[CO_3^{2-}]$, respectively. All hydrated samples show similar bands, suggesting very similar reaction products. The structure of molecular water is identified by the bending vibra-

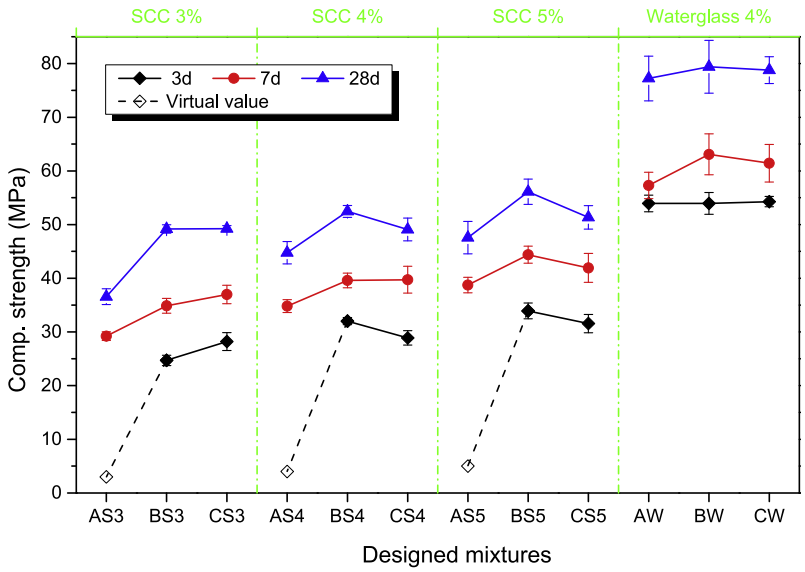

Fig. 6. Compressive strength of samples activated by sodium carbonate and waterglass with different concentrations at different curing ages (Table 3).

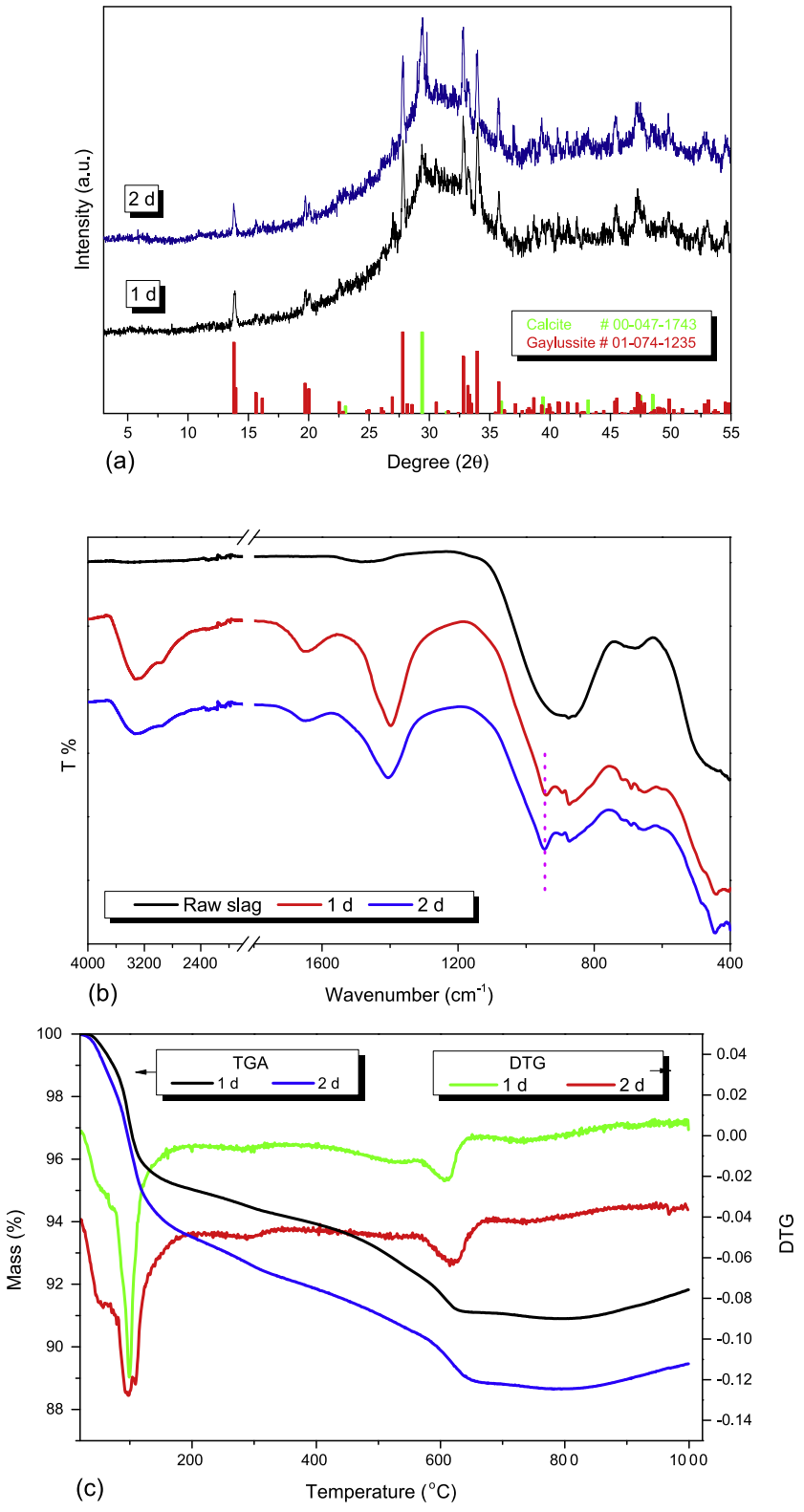

45

Fig. 7. Characterization of mixture CS5: (a) XRD, (b) FT-IR and (c) TGA-DTG.

tions located at about 3300 cm^{-1} and 1646 cm^{-1}. After mixing with activator, the vibration of Si-O bands in the SiO_4 groups shifted to a higher range at 945 cm^{-1} which is generally considered to be the consequence of the formation of calcium aluminosilicate hydrate, a C-(A)-S-H type gel [35,49]. Moreover, the intensity of band at 945 cm^{-1} increases with the increase of reaction time, indicating the ongoing generation of C-(A)-S-H gel. On the other hand, the vibration of $\upsilon_3[CO_3^{2-}]$ and Al-O bands in the AlO_4 groups

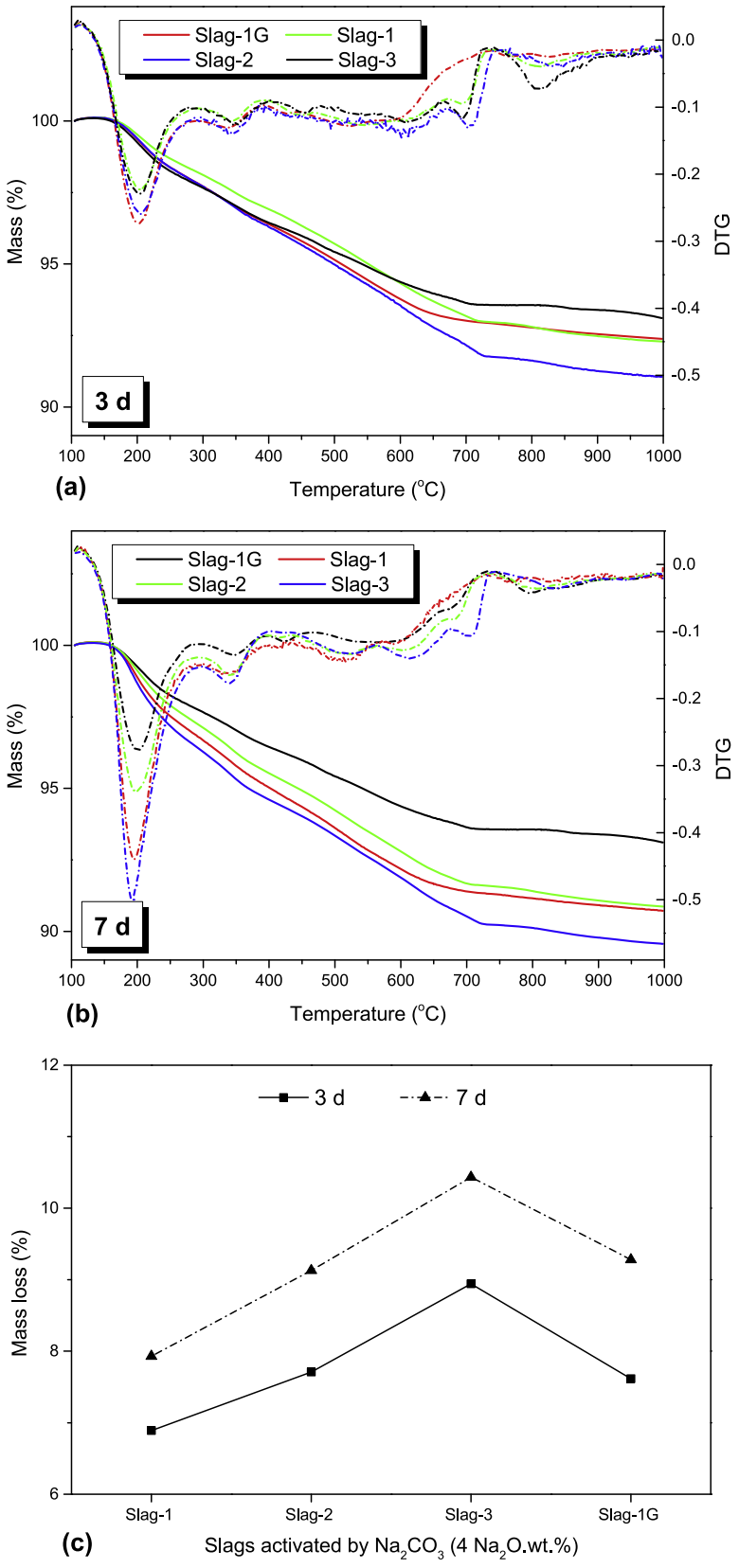

Fig. 8. Mass loss of mixtures (Table 3) during the temperature of 105–1000 °C: at the curing ages of (a) 3 d and (b) 7 d, and (c) summarized results.

shifted to lower bands at approximate 1400 cm^{-1} and 646 cm^{-1}, respectively, which could potentially attribute to the formation of new phases, e.g. gaylussite and C-(A)-S-H gel.

Fig. 7c depicts the TGA and DTG results at the curing ages of 1 d and 2 d. Both patterns show similar trends that firstly the mass decreases with the increase of temperature due to the evaporation

of free water or bound water or decompositions of minerals such as gaylussite and C-(A)-S-H gel as identified by XRD and FT-IR, and then increases after about 800 °C when further increasing the temperature possibly due to the nitriding process of the unreacted slag particles. The small shoulder appeared at approximately 50 °C is possibly to be the dehydration of C-(A)-S-H gel or potentially sodium carbonate groups (natron, trona or thermonatrite) but it is not confirmed by XRD results. Beyond 200 °C, the main decomposition happened at around 609 °C which is generally assigned to the decomposition of calcite, releasing CO_2. The small peak at about 730 °C is also the carbonate decomposition, which is contributed by gaylussite after its first dehydration happened before 200 °C [50]. The thermal peaks at around 280 °C and 529 °C could potentially be attributed to the decomposition of hydrotalcite [12,51], however, the formation of this phase is not supported by the XRD results. A possible reason is its low concentration or poor crystallization at the early age.

In previous study [48], we have found that the transformation of initially precipitated $CaCO_3$ to other phases is the key of restarting the reaction. Considering the above analysis of mixture CS5 with finer slag, one possible explanation of the accelerated reaction process is that: by increasing the fineness, more slag particles can be dissolved at the early age. Consequently, more Ca^{2+} ions are available and quickly precipitated with CO_3^{2-} anions generating calcite, gaylussite or hydrotalcite as confirmed by XRD and TGA results. When the slag fineness reaches the critical value that enough CO_3^{2-} anions can be consumed, the long dormant period will be shortened to some extent and the C-(A)-S-H gel is precipitated as supported by the FT-IR results.

It has been reported that the main reaction products of sodium carbonate activated slag at the early ages are gaylussite, different polymorphous of calcium carbonate and C-(A)-S-H gel [30,38,48]. As a result, the mass loss during the temperature 105–1000 °C is mainly due to the release of chemically bonded water and CO_2 from calcium carbonate, which can potentially give an indication about the reaction degree of sodium carbonate. The thermogravimetric analyse of the mixes (AS4, BS4 and CS4) at the ages of 3 d and 7 d are performed and the results are shown in Fig. 8. As can be seen, the mass loss increases with the increase of the particle size/fineness of slags to a certain degree and then decrease. In general, with a finer slag the mass loss is higher, indicating a higher degree of reaction. This is expected as more slag particles can be dissolved at the early stage, consequently leading to a higher degree of the dissolution of raw materials and thus the precipitation of strength-giving phase. However, when the slag fineness is over a certain limit, a faster reaction is observed but with a low reaction degree, probably due to the insufficient alkali activation caused by the low flowability.

3.6. Influential factors on Na_2CO_3 activated slag

Slow reaction of sodium carbonate activated slag has been extensively discussed. Jimenez et al. [8] investigated the effect of alkali nature on the setting time and reported that the initial precipitation of calcium carbonate is responsible for the delayed reaction process. Afterwards, limited attention has been paid to the reaction of SCAS [18,28] until recently [8,28,33,52]. Bernal et al. [30] proposed a conceptual description, stating that when the CO_3^{2-} concentration is reduced to a certain level, the formation of C-A-S-H starts and the subsequent reaction is similar as NaOH activated slag. By applying calcined layered double hydroxides (CLDH), Ke et al. [38] found that the slag pastes can set within 24 h after incorporating up to 10% of CLDH.

As can be seen from Fig. 4, the alkali dosages are more crucial on the reaction when the fineness of slag particles is low (373 m^2/kg). However, when increasing the slag fineness to a certain degree (436–461 m^2/kg), the reaction process/TRRP is significantly improved, while the alkali dosages make no significant difference on the reaction. Nevertheless, further increasing the fineness of slag (722 m^2/kg) only slightly accelerates the reaction process, while its contribution on the reaction degree is negative as shown in Fig. 8. It should be noted that the intensity of the reaction (peak height) increases with the increase of slag fineness. On the other hand, it has been experimentally confirmed that the precipitation of strength-giving phases is corresponding to the TRRP [48]. As shown in Figs. 4 and 7, it is clear that by reducing the particle size of slags, the formation of strength-giving phases can be dramatically accelerated and a 3 d-compressive strength of around 30 MPa is reached. Nevertheless, while the early strength is mainly dominated by the fineness of slags, its contribution on the later strength development is small as all samples show relatively similar compressive strength after 7 d of curing.

It should be mentioned that the reactivity of slags could also lead to significant differences on the reaction kinetics and strength development. According to Duxson and Provis [53], the reactivity of slag particles is largely controlled by the degree of deploymerization (DP) which is calculated from free Si/free Ca, assuming that all the Mg present is in akermanite ($2CaO{\cdot}Al_2O_3{\cdot}SiO_2$) and all the Al in gehlenite ($2CaO{\cdot}MgO{\cdot}2SiO_2$). Materials with a DP of about 1.3–1.5 are generally considered to have a good depolymerisation ability. To further compare the reactivity of slags, methods (Eqs. (2) and (3)) suggested by Pal et al. [54] using the hydraulic index (HI) have been taken as well. Materials are considered to have a good reactivity if the HI from Eq. (2) is about 1.0–1.3 and >1.65 from Eq. (3). The summarized results are shown in Table 5.

$$DP = \frac{Free\ Ca}{Free\ Si} = \frac{\text{Total Ca} - \text{Ca in gehlenite} - \text{Ca in akermanite} - \text{Ca associated with S}}{\text{Total Si} - \text{Si in gehlenite} - \text{Si in akermanite}} \quad (1)$$

$$HI = \frac{n(CaO) + n(MgO)}{n(SiO_2) + n(Al_2O_3)} \quad (2)$$

$$HI = \frac{n(CaO) + 1.4(MgO) + 0.56(Al_2O_3)}{n(SiO_2)} \quad (3)$$

As can be seen from Table 5, the DP is not suitable for determining the reactivity of slag particles investigated by giving minus values or high values. On the other hand, the proposal by Pal et al. [54] seems to be more reliable. In this case, the reactivity of slag particles studied in this research were similar or slightly higher than the

Table 5
Summary of calculated reactivity of slags ("[7]^1" means slag from Ref. [7] with the fineness of 450 m^2/kg, while [7]^2 means the other slag with the fineness of 900 m^2/kg).

	Slag-1	Slag-2	Slag-3	References								
				[30]	[8]	[32]	[33]	[36]	[18]	[28]	[7]^1	[7]^2
DP (Eq. (1))	1.82	−13.64	−13.95	1.56		1.12	1.02	0.87	1.15	−1.86	1.49	1.59
HI (Eq. (2))	1.30	1.51	1.51	1.28	1.76	1.24	1.23	1.19	1.28	1.11	1.33	1.35
HI (Eq. (3))	1.89	2.20	2.20	1.81	1.97	1.71	1.73	1.76	1.60	1.66	1.85	1.87

average of literatures (Table 5). Nevertheless, though the present results clearly show the effect of slag particle sizes on the reaction kinetics, it should be noted that the influence of the chemistry of slag is much more complex and not fully understood yet. For example, with a slag fineness of 460 m^2/kg, Jimenez and Puertas [8] reported a TRRP of ~137 h, while Abdalqader et al. [32] a TRRP of 45–50 h with slag fineness of 545 m^2/kg. It seems that the critical value of slag fineness on the reaction kinetics of SCAS can be different, depending on the chemistry of investigated slag. Further study on these issues is still required.

4. Conclusions

The slag characteristics on the reaction kinetics, reaction products and mechanical properties of sodium carbonate activated slag (SCAS) are evaluated by applying slags with different finenesses and activators with different dosages. Based on the presented results, the following conclusions can be drawn:

- Slag fineness significantly influences the reaction kinetics of sodium carbonate activated slag when increasing the slag fineness to a certain degree (436–461 m^2/kg), while the alkali dosages make no significant difference on the reaction;
- The initial precipitation of $CaCO_3$ negatively affects the fresh behaviour of pastes and the influences is larger when the slag particles become finer;
- 3 d compressive strengths of about 34 MPa of SCAS are achieved with the recipes with a fine slag particle (fineness of 436 m^2/kg);
- The effect of sodium carbonate dosage (3–5 Na_2O wt.%) on the reaction kinetics and strength development is not prominent.

Acknowledgements

This research was carried out under the scheme of China Scholarship Council and with the support of Eindhoven University of Technology. Furthermore, we would like to thank the following sponsors of Building Materials research group at TU Eindhoven: Rijkswaterstaat Grote Projecten en Onderhoud, Graniet-Import Benelux, Kijlstra Betonmortel, Struyk Verwo, Attero, Enci, Rijkswaterstaat Zee en Delta – District Noord, Van Gansewinkel Minerals, BTE, V.d. Bosch Beton, Selor, GMB, Icopal, BN International, Eltomation, Knauf Gips, Hess AAC Systems, Kronos, Joma, CRH Europe Sustainable Concrete Centre, Cement & Beton Centrum, Heros, Inashco, Keim and Sirius International. We also wish to thank Dr. P. Spiesz (ENCI HeidelbergCement Benelux, The Netherlands) for his assistance in measuring the Blaine fineness of the GGBSs.

References

[1] P. Duxson, G.C. Lukey, J.L. Provis, J.S.J. van Deventer, The role of inorganic polymer technology in the development of "green concrete", Cem. Concr. Res. 37 (2007) 1590–1597, http://dx.doi.org/10.1016/j.cemconres.2007.08.018.
[2] F. Pacheco-Torgal, Z. Abdollahnejad, A.F. Camoes, M. Jamshidi, Y. Ding, Durability of alkali-activated binders: a clear advantage over Portland cement or an unproven issue?, Constr Build. Mater. 30 (2012) 400–405, http://dx.doi.org/10.1016/j.conbuildmat.2011.12.017.
[3] F. Pacheco-Torgal, J. Castro-Gomes, S. Jalali, Alkali-activated binders: a review, Constr. Build. Mater. 22 (2008) 1305–1314, http://dx.doi.org/10.1016/j.conbuildmat.2007.10.015.
[4] C. Li, H. Sun, L. Li, A review: the comparison between alkali-activated slag (Si+Ca) and metakaolin (Si+Al) cements, Cem. Concr. Res. 40 (2010) 1341–1349, http://dx.doi.org/10.1016/j.cemconres.2010.03.020.
[5] A.M. Rashad, A comprehensive overview about the influence of different additives on the properties of alkali-activated slag – a guide for civil engineer, Constr. Build. Mater. 47 (2013) 29–55, http://dx.doi.org/10.1016/j.conbuildmat.2013.04.011.
[6] F. Puertas, C. Varga, M.M. Alonso, Rheology of alkali-activated slag pastes. Effect of the nature and concentration of the activating solution, Cem. Concr. Compos. 53 (2014) 279–288, http://dx.doi.org/10.1016/j.cemconcomp.2014.07.012.
[7] A.F. Jimenez, J.G. Palomo, F. Puertas, Alkali-activated slag mortars mechanical strength behaviour, Cem. Concr. Res. 29 (1999) 1313–1321.
[8] A.F. Jimenez, F. Puertas, Setting of alkali-activated slag cement. Influence of activator nature, Adv. Cem. Res. 13 (2001) 115–121, http://dx.doi.org/10.1680/adcr.2001.13.3.115.
[9] M. Heikal, M.Y. Nassar, G. El-Sayed, S.M. Ibrahim, Physico-chemical, mechanical, microstructure and durability characteristics of alkali activated Egyptian slag, Constr. Build. Mater. 69 (2014) 60–72, http://dx.doi.org/10.1016/j.conbuildmat.2014.07.026.
[10] N.K. Lee, H.K. Lee, Setting and mechanical properties of alkali-activated fly ash/slag concrete manufactured at room temperature, Constr. Build. Mater. 47 (2013) 1201–1209, http://dx.doi.org/10.1016/j.conbuildmat.2013.05.107.
[11] S. Akcaozoglu, C. Ulu, Recycling of waste PET granules as aggregate in alkali-activated blast furnace slag/metakaolin blends, Constr. Build. Mater. 58 (2014) 31–37, http://dx.doi.org/10.1016/j.conbuildmat.2014.02.011.
[12] M. Ben Haha, B. Lothenbach, G. Le Saout, F. Winnefeld, Influence of slag chemistry on the hydration of alkali-activated blast-furnace slag – Part II: Effect of Al2O3, Cem. Concr. Res. 42 (2012) 74–83, http://dx.doi.org/10.1016/j.cemconres.2011.08.005.
[13] A.M. Rashad, Alkali-activated metakaolin: a short guide for civil engineer – an overview, Constr. Build. Mater. 41 (2013) 751–765, http://dx.doi.org/10.1016/j.conbuildmat.2012.12.030.
[14] J.G. Sanjayan, F. Collins, Microcracking and strength development of alkali activated slag concrete, Cem. Concr. Compos. 23 (2001) 345–352.
[15] M. Chi, Effects of dosage of alkali-activated solution and curing conditions on the properties and durability of alkali-activated slag concrete, Constr. Build. Mater. 35 (2012) 240–245, http://dx.doi.org/10.1016/j.conbuildmat.2012.04.005.
[16] S. Wang, K.L. Scrivener, P.L. Pratt, Factors affecting the strength of alkali-activated slag, Cem. Concr. Res. 24 (1994) 1033–1043.
[17] D. Ravikumar, N. Neithalath, Reaction kinetics in sodium silicate powder and liquid activated slag binders evaluated using isothermal calorimetry, Thermochim. Acta 546 (2012) 32–43, http://dx.doi.org/10.1016/j.tca.2012.07.010.
[18] V. Zivica, Effects of type and dosage of alkaline activator and temperature on the properties of alkali-activated slag mixtures, Constr. Build. Mater. 21 (2007) 1463–1469, http://dx.doi.org/10.1016/j.conbuildmat.2006.07.002.
[19] J.G. Jang, N.K. Lee, H.K. Lee, Fresh and hardened properties of alkali-activated fly ash/slag pastes with superplasticizers, Constr. Build. Mater. 50 (2014) 169–176, http://dx.doi.org/10.1016/j.conbuildmat.2013.09.048.
[20] F. Jin, K. Gu, A.A. Tabbaa, Strength and drying shrinkage of reactive MgO modified alkali-activated slag paste, Constr. Build. Mater. 51 (2014) 395–404, http://dx.doi.org/10.1016/j.conbuildmat.2013.10.081.
[21] M. Palacios, F. Puertas, Effect of shrinkage-reducing admixtures on the properties of alkali-activated slag mortars and pastes, Cem. Concr. Res. 37 (2007) 691–702, http://dx.doi.org/10.1016/j.cemconres.2006.11.021.
[22] N.M. Piatak, M.B. Parsons, R.R. Seal, Characteristics and environmental aspects of slag: a review, Appl. Geochem. 57 (2014) 236–266, http://dx.doi.org/10.1016/j.apgeochem.2014.04.009.
[23] H. El-Didamony, A.A. Amer, T.M. El-Sokkary, H. Abd-El-Aziz, Effect of substitution of granulated slag by air-cooled slag on the properties of alkali activated slag, Ceram. Int. 39 (2013) 171–181, http://dx.doi.org/10.1016/j.ceramint.2012.06.007.
[24] S.A. Bernal, R.S. Nicolas, R.J. Myers, R. Mejia De Gutierrez, F. Puertas, J.S.J. Van Deventer, J.L. Provis, MgO content of slag controls phase evolution and structural changes induced by accelerated carbonation in alkali-activated binders, Cem. Concr. Res. 57 (2014) 33–43, http://dx.doi.org/10.1016/j.cemconres.2013.12.003.
[25] H. Yi, G. Xu, H. Cheng, J. Wang, Y. Wan, H. Chen, An overview of utilization of steel slag, Procedia Environ. Sci. 16 (2012) 791–801, http://dx.doi.org/10.1016/j.proenv.2012.10.108.
[26] B. Yuan, Q.L. Yu, H.J.H. Brouwers, Reaction kinetics, reaction products and compressive strength of ternary activators activated slag designed by Taguchi method, Mater. Des. 86 (2015) 878–886, http://dx.doi.org/10.1016/j.matdes.2015.07.077.
[27] A.R. Sakulich, E. Anderson, C. Schauer, M.W. Barsoum, Mechanical and microstructural characterization of an alkali-activated slag/limestone fine aggregate concrete, Constr. Build. Mater. 23 (2009) 2951–2957, http://dx.doi.org/10.1016/j.conbuildmat.2009.02.022.
[28] C. Duran Atis, C. Bilim, O. Celik, O. Karahan, Influence of activator on the strength and drying shrinkage of alkali-activated slag mortar, Constr. Build. Mater. 23 (2009) 548–555, http://dx.doi.org/10.1016/j.conbuildmat.2007.10.011.
[29] T. Bakharev, J.G. Sanjayan, Y.B. Cheng, Alkali activation of Australian slag cements, Cem. Concr. Res. 29 (1999) 113–120, http://dx.doi.org/10.1016/S0008-8846(98)00170-7.
[30] S.A. Bernal, J.L. Provis, R.J. Myers, R. San Nicolas, J.S.J. van Deventer, Role of carbonates in the chemical evolution of sodium carbonate-activated slag binders, Mater. Struct. 48 (2014) 517–529, http://dx.doi.org/10.1617/s11527-014-0412-6.
[31] H. Xu, J.L. Provis, J.S.J. Van Deventer, P.V. Krivenko, Characterization of aged slag concretes, Mater. J. 105 (2008) 131–139.
[32] A.F. Abdalqader, F. Jin, A. Al-Tabbaa, Characterisation of reactive magnesia and sodium carbonate-activated fly ash/slag paste blends, Constr. Build. Mater. 93 (2015) 506–513, http://dx.doi.org/10.1016/j.conbuildmat.2015.06.015.

[33] F. Jin, K. Gu, A. Al-Tabbaa, Strength and drying shrinkage of slag paste activated by sodium carbonate and reactive MgO, Constr. Build. Mater. 51 (2014) 395–404, http://dx.doi.org/10.1016/j.conbuildmat.2013.10.081.
[34] T. Bakharev, J.G. Sanjayan, Y.B. Cheng, Effect of admixtures on properties of alkali-activated slag concrete, Cem. Concr. Res. 30 (2000) 1367–1374, http://dx.doi.org/10.1016/S0008-8846(00)00349-5.
[35] F. Puertas, M.T. Carrasco, Use of glass waste as an activator in the preparation of alkali-activated slag. Mechanical strength and paste characterisation, Cem. Concr. Res. 57 (2014) 95–104, http://dx.doi.org/10.1016/j.cemconres.2013.12.005.
[36] M. Kovtun, E.P. Kearsley, J. Shekhovtsova, Chemical acceleration of a neutral granulated blast-furnace slag activated by sodium carbonate, Cem. Concr. Res. 72 (2015) 1–9, http://dx.doi.org/10.1016/j.cemconres.2015.02.014.
[37] F. Collins, J.G. Sanjayan, Early age strength and workability of slag pastes activated by NaOH and Na2CO3, Cem. Concr. Res. 28 (1998) 655–664.
[38] X. Ke, S.A. Bernal, J.L. Provis, Controlling the reaction kinetics of sodium carbonate-activated slag cements using calcined layered double hydroxides, Cem. Concr. Res. 81 (2016) 24–37, http://dx.doi.org/10.1016/j.cemconres.2015.11.012.
[39] C. Shi, Y. Li, Investigation on some factors affecting the characteristics of alkali-phosphorus slag cement, Cem. Concr. Res. 19 (1989) 527–533, http://dx.doi.org/10.1016/0008-8846(89)90004-5.
[40] N.K. Lee, E.M. Kim, H.K. Lee, Mechanical properties and setting characteristics of geopolymer mortar using styrene-butadiene (SB) latex, Constr. Build. Mater. 113 (2016) 264–272, http://dx.doi.org/10.1016/j.conbuildmat.2016.03.055.
[41] B. Standard E. 196-1, Methods of Testing Cement Part 1: Determination of Strength, 2005.
[42] H.W. Reinhardt, Beton als Constructiemateriaal Eigenschappen en Duurzaamheid, Delftse Universitaire Pers, 1998.
[43] F. Han, R. Liu, D. Wang, P. Yan, Characteristics of the hydration heat evolution of composite binder at different hydrating temperature, Thermochim. Acta (2014), http://dx.doi.org/10.1016/j.tca.2014.04.010.
[44] X. Gao, Q.L.L. Yu, H.J.H. Brouwers, Reaction kinetics, gel character and strength of ambient temperature cured alkali activated slag-fly ash blends, Constr. Build. Mater. 80 (2015) 105–115, http://dx.doi.org/10.1016/j.conbuildmat.2015.01.065.
[45] A.M. Rashad, Y. Bai, P.A.M. Basheer, N.B. Milestone, N.C. Collier, Hydration and properties of sodium sulfate activated slag, Cem. Concr. Compos. 37 (2013) 20–29, http://dx.doi.org/10.1016/j.cemconcomp.2012.12.010.
[46] K. Yang, J. Song, Workability loss and compressive strength development of cementless mortars activated by combination of sodium silicate and sodium hydroxide, J. Mater. Civ. Eng. 21 (2009) 119–127.
[47] B. Yuan, Q.L. Yu, H.J.H. Brouwers, Investigation on the activating effect of Na_2CO_3 and NaOH on slag, in: Proc. Int. Conf. Non-Traditional Cem. Concr., 2014, pp. 21–25.
[48] B. Yuan, Q.L. Yu, H.J.H. Brouwers, Time-dependent characterization of Na_2CO_3 activated slag, Cem. Concr. Compos. (2015) (submitted for publication).
[49] F. Puertas, M. Palacios, H. Manzano, J.S. Dolado, A. Rico, J. Rodriguez, A model for the C-A-S-H gel formed in alkali-activated slag cements, J. Eur. Ceram. Soc. 31 (2011) 2043–2056, http://dx.doi.org/10.1016/j.jeurceramsoc.2011.04.036.
[50] D.R. Jornson, W.A. Ross, Gaylussite: thermal properties by simultaneous thermal analysis, Am. Mineral. 58 (1973) 778–784.
[51] V. Vagvolgyi, S.J. Palmer, J. Kristof, R.L. Frost, E. Horvath, Mechanism for hydrotalcite decomposition: a controlled rate thermal analysis study, J. Colloid Interface Sci. 318 (2008) 302–308, http://dx.doi.org/10.1016/j.jcis.2007.10.033.
[52] A.J. Moseson, D.E. Moseson, M.W. Barsoum, High volume limestone alkali-activated cement developed by design of experiment, Cem. Concr. Compos. 34 (2012) 328–336, http://dx.doi.org/10.1016/j.cemconcomp.2011.11.004.
[53] P. Duxson, J.L. Provis, Designing precursors for geopolymer cements, J. Am. Ceram. Soc. 91 (2008) 3864–3869, http://dx.doi.org/10.1111/j.1551-2916.2008.02787.x.
[54] S. Pal, A. Mukherjee, S. Pathak, Investigation of hydraulic activity of ground granulated blast furnace slag in concrete, Cem. Concr. Res. 33 (2003) 1481–1486, http://dx.doi.org/10.1016/S0008-8846(03)00062-0.